Carbohydrate Polymers 87 (2012) 1941–1949

Contents lists available at SciVerse ScienceDirect

Carbohydrate Polymers

journal homepage: www.elsevier.com/locate/carbpol

New insights on the mechanism of acid degradation of pea starch

Shujun Wang[a], Jaroslav Blazek[b], Elliot Gilbert[b,*], Les Copeland[a,**]

[a] Faculty of Agriculture, Food and Natural Resources, University of Sydney, NSW 2006, Australia
[b] Bragg Institute, Australian Nuclear Science and Technology Organisation, Locked Bag 2001, Kirrawee DSC, NSW 2232, Australia

ARTICLE INFO

Article history:
Received 4 August 2011
Received in revised form 3 September 2011
Accepted 30 September 2011
Available online 6 October 2011

Keywords:
Starch
Acid hydrolysis
Distribution of amylose
Granule organization

ABSTRACT

The degradation of pea starch granules by acid hydrolysis has been investigated using a range of chemical and structural methods, namely through measuring changes in amylose content by both the iodine binding and concanavalin A precipitation methods, along with small angle X-ray scattering (SAXS), wide angle X-ray diffraction (XRD) and field emission scanning electron microscopy (FE-SEM). The relative crystallinity, intensity of the lamellar peak and the low-*q* scattering increased during the initial stages of acid hydrolysis, indicating early degradation of the amorphous regions (growth rings and lamellae). In the first 2 days of hydrolysis, there was a rapid decline in amylose content, a concomitant loss of precipitability of amylopectin by concanavalin A, and damage to the surface and internal granular structures was evident. These observations are consistent with both amylose and amylopectin being located on the surface of the granules and attacked simultaneously in the early stages of acid hydrolysis. The results are also consistent with amylose being more concentrated at the core of the granules. More extensive hydrolysis resulted in the simultaneous disruption of amorphous and crystalline regions, which was indicated by a decrease in lamellar peak intensity, decrease in interhelix peak intensity and no further increase in crystallinity. These results provide new insights into the organization of starch granules.

1. Introduction

Starch is an important polysaccharide for humans. It is a major source of dietary carbohydrates and energy and is used industrially in many food and non-food applications. Starch is deposited in plants in the form of insoluble, semi-crystalline granules, which are made up of the two polymers of α-D-glucopyranose, amylose and amylopectin. Amylose is an essentially linear α(1→4) glucan that accounts for 20–35% by weight of most starches, whereas amylopectin is a highly branched polymer with α(1→4) glycosidic linkages and 2–5% of the glucoses in α(1→6) glucosyl bonds. The amylose content, structure of amylopectin and organization of these molecules within the granule determine the functional properties that are important in food processing and nutrition, such as water absorption, pasting and viscosity, gelatinization and retrogradation. Currently, the generally accepted model for the organization of starch granules is that they have alternating concentric semicrystalline and amorphous growth rings of similar thickness, between about 120 to 400 nm thick (Buléon, Colonna, Planchot, & Ball, 1998; Pérez & Bertoft, 2010). The semicrystalline growth rings consist of alternating crystalline and amorphous lamellae with a repeat period of 9–10 nm (Oostergetel & van Bruggen, 1989). The crystalline lamellae are considered to be formed by the arrangement of double helical configurations of external short, branched chains of amylopectin (mainly A and B_1 chains), into clusters that pack into A- or B- type crystalline polymorphs (Buléon et al., 1998). The amorphous regions are considered to contain much of the amylose and amylopectin branch points and chains not organized into helical configurations. Cereal grain starches contain predominantly A-type crystallites, whereas B-type crystallites are present mostly in root and tuber starches as well as high-amylose starches. An intermediate type of crystal polymorph, which includes both A- and B-type crystallites and is termed C-type, occurs in starch from some legumes, rhizomes and fruits (Bogracheva, Morris, Ring, & Hedley, 1998; Cairns, Bogracheva, Ring, Hedley, & Morris, 1997; Stevenson, Domoto, & Jane, 2006; Wang, Yu, Chen, & Liu, 2008; Wang, Yu, Yu, et al., 2008; Wang, Sharp, & Copeland, 2011).

Examination of the orientation of the polymer chains in potato starch using microfocus X-ray diffraction showed that the peripheral regions of the granules were more highly organized than the internal regions and hilum (Buléon et al., 1997; Waigh, Hopkinson, & Donald, 1997). Accordingly, Ziegler, Creek, & Runt, 2005 proposed that there is an amorphous or less-crystalline region between the hilum and the peripheral growth rings. Structural changes observed in pea and Chinese yam starch granules

* Corresponding author. Tel.: +61 2 9717 9470; fax: +61 2 9717 3606.
** Corresponding author. Tel.: +61 2 8627 1017; fax: +61 2 8627 1099.
E-mail addresses: elliot.gilbert@ansto.gov.au (E. Gilbert), les.copeland@sydney.edu.au (L. Copeland).

0144-8617/$ – see front matter © 2011 Elsevier Ltd. All rights reserved.
doi:10.1016/j.carbpol.2011.09.093

subjected to acid hydrolysis were consistent with this proposal (Wang, Yu, & Yu, 2008a, 2008b; Wang, Yu, Zhu, Yu, & Jin, 2009). However, little work has been directed at examining the amorphous growth rings and central amorphous core of granules, except the proposed hypothesis that a large portion of amylose resides in amorphous growth rings (Jenkins & Donald, 1995).

The relative location of amylose and amylopectin in native starch granules continues to be a matter of debate. Amylose was proposed to be located in bundles among amylopectin clusters in amorphous regions (Nikuni, 1978). However, experiments with cross-linking agents on potato and corn starch, were interpreted as showing that individual amylose molecules are interspersed among the amylopectin molecules rather than grouped together (Jane, Xu, Radosavljevic, & Seib, 1992). Chemical surface-gelatinization of potato and normal maize starches further indicated that amylose is more concentrated at the periphery than at the core of the granules (Jane & Shen, 1992). On the other hand, on the basis of iodine staining, the amylose component of transgenic potato starches has been proposed to be synthesised within the matrix formed by amylopectin and largely confined to a central region of the granule (Tatge, Marshall, Martin, Edwards, & Smith, 1999).

Analysis of granules that have been partially hydrolysed by acid has also been used extensively as an approach to reveal the structure of starch granules. Interest in the effects of acid on starch is also of relevance because of their industrial significance. Acid-hydrolyzed starch has been used extensively in the food, pharmaceutical, paper and textile industries and in biodegradable plastics (Hoover, 2000; Le Corre, Bras, & Dufresne, 2010). X-ray diffraction studies have shown that acid hydrolysis initially increases the crystallinity of granules, which has been taken to indicate preferential initial attack in the amorphous regions. This has also been confirmed by SAXS, which showed that the lamellar peak becomes less pronounced upon hydrolysis (Jenkins & Donald, 1997; Oostergetel & van Bruggen, 1989). Due to the abundance of amylose in the amorphous regions, amylose has been hypothesized to be hydrolysed more readily than amylopectin (Biliaderis, Grant, & Vose, 1981). However, direct evidence for the mode of degradation of amylose and amylopectin is limited. The objectives of the present study are to use a combination of methods to measure acid hydrolysis-induced changes in granules (amylose content, wide angle X-ray diffraction, small angle X-ray scattering, high magnification imaging) to clarify whether there is a preferential hydrolytic attack on amylose or amylopectin, and in the amorphous or crystalline regions, and to provide new insights into the distribution of amylose and amylopectin within the granules. The thermal transitions of acid-hydrolysed pea starch are described in an accompanying paper (Wang & Copeland, 2011).

2. Experimental

2.1. Materials

Three varieties of field pea varieties (Maki, Kaspa, PRL131) were obtained from the Plant Breeding Institute of The University of Sydney. The source of these varieties is described in Wang et al. (2011). Starch was isolated according to the method of Wang et al. (2011). The moisture contents of the isolated starches were 11.1% (Maki), 11.8% (Kaspa) and 11.4% (PRL131), and the amylose contents were between 35 and 38%. Enzyme kits for total starch and amylose/amylopectin determination were purchased from Megazyme International Ireland Ltd. (Bray, Co. Wicklow, Ireland).

2.2. Preparation of acid-hydrolyzed starches

The acid-hydrolyzed starches were prepared according to the method of Wang et al. (2008b) with minor modifications. This is similar to the method used generally to prepare Lintnerized starches (Robin, Mercier, Charbonniere, & Guilbot, 1974). Six separate samples of native starch (10 g dry basis) were each suspended in 100 mL of 2.2 mol/L HCl solution and kept at 36 °C. The mixtures were shaken intermittently by hand during the hydrolysis period. Samples were taken after 1, 2, 6, 12, 20 and 35 days and filtered through Whatman No. 1 filter paper with suction. The residue was washed with distilled water until the filtrate was at neutral pH and then twice with 95% ethanol. The resulting acid-hydrolyzed starch residue was dried overnight at room temperature under a gentle air stream, and ground to pass through a 100 mesh sieve. The yield of the acid-hydrolyzed starch was calculated from weight of starch (dry basis) after acid hydrolysis divided by the weight of starch (dry basis) before hydrolysis.

2.3. Amylose content

Native and acid-treated starches were defatted with aqueous methanol (85%, v/v) for 30 min at 60 °C and the amylose content was determined by the iodine binding colorimetric method (Williams, Kuzina, & Hlynka, 1970) and the concanavalin A (Con A) method using the Megazyme Amylose/Amylopectin Assay Kit according to the manufacturer's instructions.

2.4. Small-angle X-ray scattering (SAXS) measurements

SAXS measurements were obtained using a Bruker NanoStar SAXS instrument equipped with Vantec 2000 area detector (effective pixel size 54 μm) and pin-hole collimation for point focus geometry. The X-ray source was a copper rotating anode (0.3 mm filament) operating at 45 kV and 110 mA, fitted with cross coupled Göbel mirrors, resulting in a Cu Kα radiation wavelength of 1.5418 Å. The optics and sample chamber were under vacuum to minimize air scattering. The sample to detector distance was chosen to be 700 mm, which provided a q-range from 0.14 to 4.30 nm^{-1}. The q resolution of the instrument at the main lamellar peak at ca. 0.6 nm^{-1} was calculated to be 0.01 nm^{-1}. Samples were presented in 2 mm sealed quartz capillaries as suspensions containing excess water above the sedimented sample and scattering was measured for 60 min. A sealed 2 mm quartz capillary filled with water was used as a background. SAXS datasets were radially averaged using Bruker AXS software 4.1.30. SAXS curves were normalized to sample transmission and background-subtracted using Igor software (Wavemetrics, Lake Oswego, OR, USA).

Scattering data were fitted to a function as described previously representing a combination of a power-law term and multiple peaks (Blazek & Gilbert, 2010). The power-law function accounts for the scattering arising from structures of larger length-scale than lamellae including interfaces. The lamellar peak around 0.6 nm^{-1} was fitted to the function comprising the sum of a Lorentzian peak and a Gaussian peak with identical peak centre, intensity and width. A second reflection peak around 1.2 nm^{-1}, where applicable, was fitted to a single Gaussian peak. The overall equation is as follows:

$$I(q) = k \cdot \frac{I_{01}}{1 + (2(q - q_{01})/B_1)^2} + (1 - k) \cdot I_{01} \exp\left[-\frac{(q - q_{01})^2}{2B_1^2}\right] + I_{02} \exp\left[-\frac{(q - q_{02})^2}{2B_2^2}\right] + Aq^{-\delta} + Bkgd$$

where the first term is a Lorentzian function and the second is a Gaussian in which I_0 is the peak height, q_0 is the position of

centre of the peak, and the B term is related to the full width at half maximum of the peak. The third term is the Gaussian peak, which fits the second order reflection. The fourth term represents a power-law where A is the prefactor and δ is the exponent of the power-law function. The Bragg spacing d was calculated from the position of the peak according to $d = 2\pi/q_0$. However, as found in some previous studies investigating B-type starches (e.g. Blazek & Gilbert, 2010), this approach understates the complexity of starch structure. Indeed, there is substantial evidence for the presence of structures intermediate in dimension to the lamellae and growth rings. These blocklet, and perhaps superhelical structures (Baldwin, Adler, Davies, & Melia, 1998; Pérez & Bertoft, 2010) are likely to influence the observed low q behaviour in addition to granular interfacial scattering. To address the latter, a further Gaussian peak has been incorporated into the fitting function. Its behaviour as a function of hydrolysis time is discussed below.

2.5. X-ray diffraction (XRD) measurements

XRD patterns from the powders were obtained using a Bruker D8 Focus X-ray diffractometer (Bruker AXS, Germany) with a Cu Kα source (λ = 0.154 nm) running at 40 kV and 40 mA. The specimens were stored in a desiccator over a saturated solution of NaCl in a constant humidity atmosphere of 75% for 1 week before spectra were collected. The moisture content was roughly estimated to be 30% according to Bogracheva, Wang, Wang & Hedley, 2002. The intensity was measured from 4 to 35° as a function of 2θ and at a scanning speed of 0.5°/min and a step size of 0.04°. Relative crystallinity of the samples was quantified according to the method of Wang, Yu, Yu, et al. (2008).

2.6. Field-emission scanning electron microscopy (FE-SEM)

Native and acid-hydrolyzed field pea starches were fixed onto the surface of double-sided, carbon-coated adhesive tape attached to an aluminium stub. The mounted starch granules were coated with palladium/gold prior to imaging in a field emission scanning electron microscope (Carl Zeiss ULTRA plus, Germany). The accelerating voltage was 1.01 kV and the magnification is shown on the micrographs.

3. Results

3.1. Recovery of starch

All of the starches exhibited a similar hydrolysis pattern, in which approximately 45% of the starch was solubilised during the first 6 days, followed by an additional 35% of the starch solubilised between 6 and 35 days (Fig. 1). Thus, after 35 days of hydrolysis, about 20% of the starch was recoverable by filtration, and 80% had been solubilised. As no significant differences were observed between the three starch varieties, only the results obtained with variety Maki are presented subsequently.

3.2. Changes in amylose content

The changes in amylose content of acid-hydrolysed starch, as measured by iodine binding, are presented in Fig. 2. As hydrolysis time increased, a progressive decrease in amylose content was observed, from about 34% in native starch to 25% in starch hydrolyzed for 1 day, and to 8% after 2 days of hydrolysis. After 6 days of acid hydrolysis, the absorbance value of the residual starch mixed with iodine was lower than that of pure amylopectin indicating that the chain length of any residual amylose was too short to form a blue iodine complex. For comparison, amylose content in these acid-hydrolyzed starches was taken as zero.

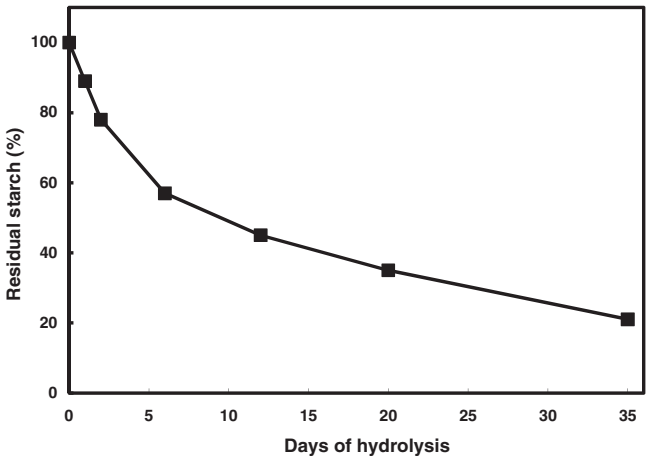

Fig. 1. Recovery of residual starch after acid hydrolysis. The recovery of starch after acid hydrolysis was calculated from weight of starch (dry basis) after filtration and washing as described in section 2.2.

A completely opposite trend was observed when amylose content was determined by the Con A method, which depends on the ability of Con A to form a precipitate with amylopectin (Fig. 2). The increase in apparent amylose content of the acid-hydrolyzed starches to 55%, 88% and 100% after 1, 2 and 6 days of hydrolysis, as measured by the Con A method (Fig. 2), is indicative of the progressive loss of binding affinity and/or precipitability of Con A with acid-damaged amylopectin, not increasing amylose content. For acid-hydrolyzed starch, the amylose content measured by Con A is thus overestimated as a result of amylopectin molecules with degraded branch points having lost the ability to form a precipitate with Con A.

3.3. Crystallinity

The XRD spectra and changes in relative crystallinity are shown in Fig. 3. Relative crystallinity increased rapidly from 48% to about 64% during the first 6 days of acid hydrolysis, after which it did not change significantly (Fig. 3). The increase in crystallinity, which was evident from the increase in intensity of the dominant diffraction peaks relative to the whole spectrum (Fig. 3). It is interesting to

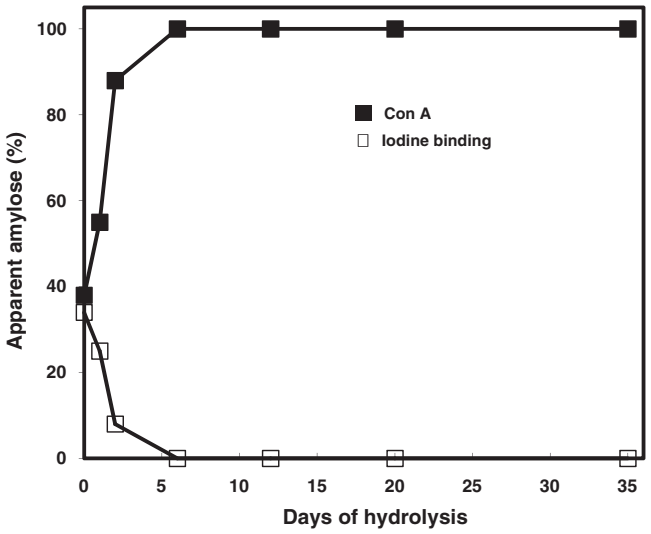

Fig. 2. Effect of hydrolysis on apparent amylose content of native and acid-hydrolysed starch granules as determined by the iodine binding and Con A methods, as described in section 2.3.

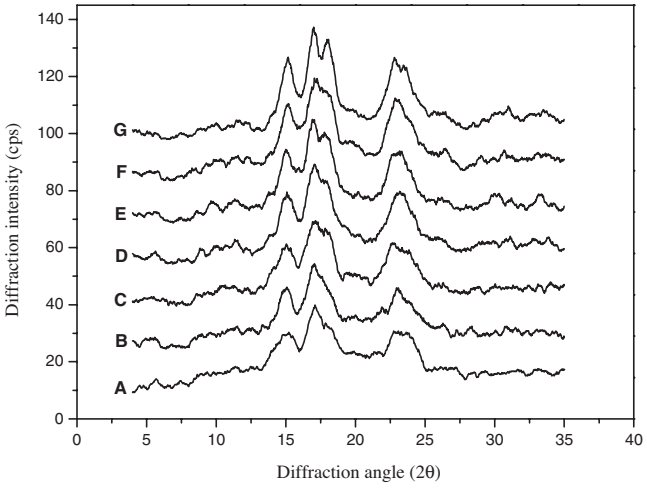

Fig. 3. X-ray diffraction spectra of native and acid-hydrolysed starches. The spectra for native starch (A), and starch residues after hydrolysis for 1 (B), 2 (C), 6 (D), 12 (E), 20 (F) and 35 days (G) have been offset for clarity.

note that there are qualitative differences in the XRD spectra in the region of 17–18° 2θ. Native starch showed a peak with a shoulder in this part of the spectrum, whereas two well separated peaks were evident in the spectrum of starch hydrolysed for 35 days. The peak at 17.0° 2θ in the spectrum occurs for both A- and B-type crystalline polymorphs, whereas the peak at 17.9° 2θ is characteristic of only the A-type polymorph (Bogracheva et al., 1998; Cairns et al., 1997). The shoulder peak at 17.9° 2θ became more pronounced over time (Fig. 3), indicating that the A-polymorph is abundant in the acid-hydrolysed starch after 35 days of acid hydrolysis. Due to the low signal-to-noise ratio of the XRD patterns, the degree of crystallinity was not calculated using a curve fitting procedure such as that described by Lopez-Rubio, Flanagan, Gilbert, and Gidley (2008), and hence the relative proportion of A/B polymorphs was not determined.

3.4. SAXS

The application of SAXS to investigate starch structure has recently been reviewed (Blazek & Gilbert, 2011). Native starch granules from the three pea varieties used in this study gave similar SAXS patterns (Fig. 4a). The scattering patterns were characterised by intense scattering at low scattering vector (q), which rapidly decreased at larger angles and featured three scattering peaks: a well-resolved main peak around q of ca. 0.60 nm^{-1} (arising from a periodic arrangement of alternating crystalline and amorphous lamellae, corresponding to Bragg spacing of 10.4 nm); a broad weak second order reflection peak at about 1.2 nm^{-1} (corresponding to a Bragg spacing of 5.8 nm); and the 100 interhelix peak around 3.9 nm^{-1} (corresponding to the distance between the 100 crystallographic planes in the hexagonal unit cell of B-crystalline starch).

Native Maki pea starch was characterised by well-defined lamellar peak positioned at 0.60 nm^{-1} with intensity of ca. 2100 relative units (r.u.) and 100 interhelix peak at 3.9 nm^{-1} with intensity of 49 r.u. Acid hydrolysis had a significant effect on the scattering patterns from the pea starches examined in this study (Fig. 4b). The lamellar peak in the native starch gradually increased in intensity in the first 2 days of hydrolysis (to ca. 9000 r.u.), after which it decreased to the point when it was barely evident after 35 days of hydrolysis (ca. 700 r.u.). The position of the lamellar peak was approximately constant within experimental error within the first 6–12 days of hydrolysis with the peak centre shifting gradually to higher q (lamellar spacing decreased to ca. 8.4 nm) after 35 days of hydrolysis. The lamellar peak width gradually broadened during

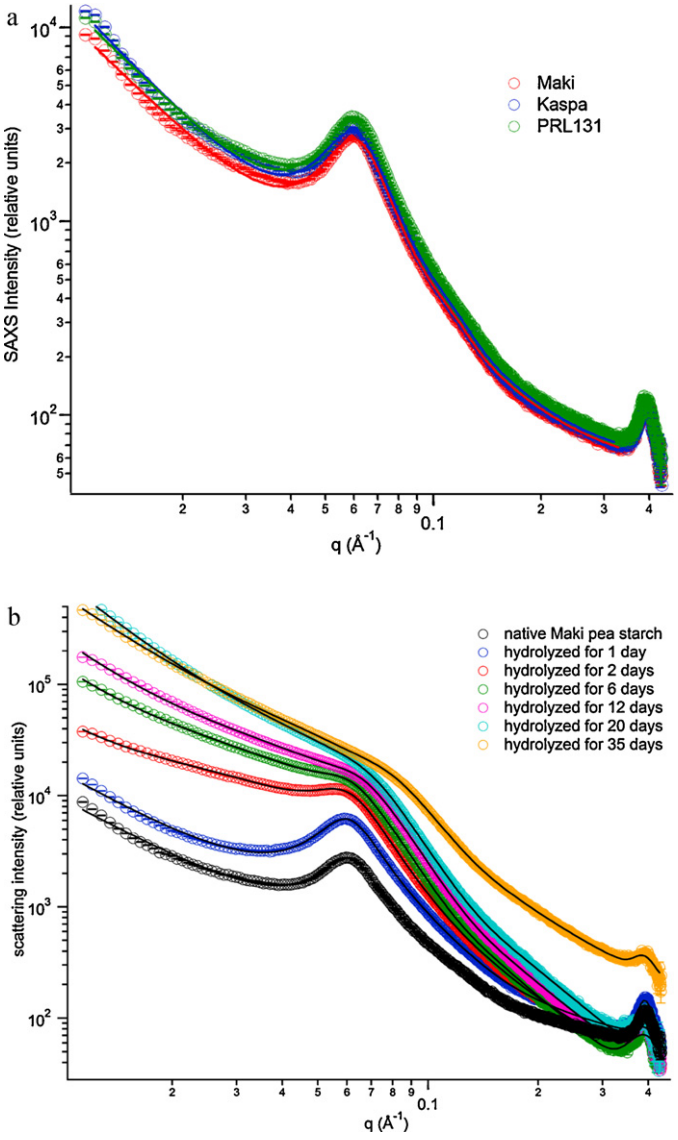

Fig. 4. (a) SAXS patterns of native pea starches used in this study. (b) Effect of acid hydrolysis on the SAXS pattern from Maki pea starch. Solid lines represent the best fits to the experimental data.

the course of acid hydrolysis (from 0.23 to 0.48 nm^{-1}). Our results for the changes in the lamellar features (Table 1) are in general agreement with data published by Oostergetel and van Bruggen (1989) and Jenkins and Donald (1997) who showed that the lamellar peak intensity increased during early stages of acid hydrolysis, followed by a decrease in the later stages of hydrolysis. However, further features are apparent in our data. It is noteworthy that the interhelix repeat is poorly defined in the XRD but has a strong intensity in the SAXS. The strong interhelix signal in the SAXS exhibits its maximum intensity at day 1 and then decreases as a function of hydrolysis time, suggesting the gradual reduction in the number of interhelical repeats. The width also broadens (up to 20 d) indicating a reduction in long range order. As discussed above, a further Gaussian function, was also required to address additional scattering in the low q region. This low-q scattering increased up to 6 days of hydrolysis, after which it decreased somewhat, although the intensity remained higher than that of native starch. In addition, the peak centre decreased from ca. 0.4 to 0 nm^{-1} in 6 days and remained centred at zero for the remainder of hydrolysis time. This suggests that structures, larger in size to the semi-crystalline lamellae, increase

Table 1
Structural parameters of Maki pea starch after acid hydrolysis. SAXS peak fitting parameters represent best fits of a power-law function plus a Gaussian-Lorentzian function to the lamellar peak as described in the text. The lamellar peak intensity is in relative units (r.u.). The SAXS instrument resolution at q of 0.6 nm^{-1} was *ca* 0.01 nm^{-1}, and the uncertainty from fitting the parameters was much smaller than this value. Values in brackets indicate uncertainty from the fitting algorithm.

	Native	1 day	2 days	6 days	12 days	20 days	35 days
Recovery yield (%)	100	89	78	57	45	35	21
Crystallinity (%)	48	54	60	64	68	69	68
Lamellar peak intensity (r.u.)	2123(5)	4278(8)	8950(40)	5170(20)	3570(20)	1550(20)	750(30)
Lamellar peak position (nm^{-1})	0.60	0.60	0.58	0.60	0.62	0.63	0.75
Lamellar peak spacing (nm)	10.4	10.5	10.8	10.5	10.1	9.9	8.4
Lamellar peak width (nm^{-1})	0.23	0.26	0.33	0.32	0.36	0.35	0.48
100 interhelix peak intensity (r.u.)	48.6(6)	59.1(6)	44.6(5)	31.8(4)	25.8(3)	16.8(3)	17.2(5)
Powerlaw exponent	1.82	1.90	2.81	2.48	2.59	2.81	2.29

in dimension within the first 6 days but are subsequently disrupted or reduce in scattering contrast.

3.5. Starch granule morphology

The surface of native starch granules appeared to be smooth when viewed at 2000× magnification. The granules had indentations or grooves (indicated by white arrow in Fig. 5A1), but there was no evidence of fissures or pores. Interestingly, the roughening of the starch granule surface could be clearly observed at high magnification (Fig. 5A2), where starch chains appeared to be tightly compacted to form the small indentations and protrusions. The rough surface may correspond to amylopectin clusters that have been observed by atomic force microscopy and low voltage SEM studies (Baldwin, Davies, & Melia, 1997; Dang, Braet, & Copeland, 2006). After 1 or 2 days of acid treatment, the starch granules at low magnification did not appear greatly changed from the native granules, apart from evidence of cracks appearing on the surface (indicated by white arrows in Fig. 5B1 and C1), which increased after 6 days (Fig. 5D1). However, images taken at high magnification indicated that after 1 day of acid hydrolysis the outer surface of the granule had a more open, lace-like appearance that was clearly indicative of the hydrolytic damage to some of the clusters (Fig. 5B2). There was evidence of extensive pitting on the inner surface covered by lace-like structure, and of small dark spots that may represent the formation of pores or channels (Fig. 5B2). Deeper etching of the surface and more extensive cracks and pores were evident after 2 and 6 days of hydrolysis (Fig. 5C2 and D2). The surface of the granule appeared to have been etched into many connected ridges and valleys, with darkened areas corresponding to deeper indentations beginning to appear. After 6 days of hydrolysis, some of the starch granules had ruptured (Fig. 5D1) and the network of ridges on the surface had essentially disappeared as a result of severe corrosion (Fig. 5D2). Nevertheless, at low magnification most of the granules observed were still clearly recognisable as having their original granular form. On exposure to acid for 12 days and beyond, the starch granules were severely corroded and few remained intact (data not shown).

Fig. 6a highlights a granule that has split open after 2 days of hydrolysis; it shows a well-defined concentric growth-ring structure surrounding less organized core material at the centre of the granule. Similar structures were also observed in other studies of native, acid-treated and enzyme-treated pea starches (Ridout, Parker, Hedley, Bogracheva, & Morris, 2006; Wang et al., 2008a). Channels (white arrow in Fig. 6a) from the surface into the core were clearly visible and the core showed evidence of major damage. Two types of concentric structures were evident: (i) rings with a solid appearance that were estimated from the micrograph to decrease gradually in thickness from 450–550 nm for those closer to the core, to 80–160 nm for rings near the periphery and (ii) rings with a less dense appearance that were more uniform and 60–80 nm in thickness. In view of their relative intactness, it was concluded that the solid rings were semi-crystalline and mainly composed of organized amylopectin side chain clusters. The narrower, indented rings are proposed to be amorphous growth rings, which could be formed by some amylose chains interspersed within amylopectin and extended chains of amylopectin that interconnect the clusters. The width of these amorphous growth rings (approximately 60–80 nm) is much smaller than that of semi-crystalline growth rings proximal to the core, but comparable with the distal ones, which is consistent with the findings of Li, Vasanthan, Hoover, and Rossnagel (2003).

4. Discussion

4.1. Degradation mode of amylose and amylopectin

The present study has shown that amylose content, as determined by iodine binding, decreased greatly in the early stage of hydrolysis. An early decrease in amylose content has also been reported by others and interpreted as indicating preferential hydrolysis of amorphous regions (Atichokudomchai, Varavinit, & Chinachoti, 2002; Biliaderis et al., 1981). Based on SAXS data, Jenkins and Donald (1995) proposed that amylose is largely located in the amorphous regions (growth rings) of starch granules. Hence, it is plausible to suggest that preferential acid attack in the amorphous regions leads to hydrolysis of amylose, consistent with the observed decrease in amylose content. The amorphous regions are generally considered to also contain amylopectin α-(1→6) branch points, which would be degraded concomitantly with amylose in the early stage of acid hydrolysis. Using the iodine binding method, Betancur and Chel (1997) found that the amylose content increased initially on acid hydrolysis; which they ascribed to a faster rate of depolymerisation of amylopectin than amylose resulting in an increased amount of linear chains.

In contrast, the apparent amylose content, as determined by the Con A binding method, increased rapidly during the initial stages of acid hydrolysis. The interaction of Con A with carbohydrates to form a precipitate occurs only with highly branched polysaccharides that contain α-D-glucopyranosyl or α-D-mannopyranosyl residues at non-reducing ends. The binding affinity of Con A for α-D-glucans has been shown to be largely dependent on the degree of branching (Goldstein, Hollerman, & Merrick, 1965), hydrodynamic volume and external chain length of branched polysaccharides (Colonna, Biton, & Mercier, 1985). The initial rapid increase in apparent amylose content is proposed to be an overestimation attributed to a significant loss of precipitability as a result of Con A binding affinity for amylopectin molecules that have insufficient non-reducing ends per molecule or short external chains due to the depolymerisation of amylopectin in amorphous regions. An increase in apparent amylose content, as measured by the Con A method, was also observed with high-amylose maize starch by Li, Corke, and Beta (2007), who interpreted the result as indicating preferential hydrolysis of amylopectin, which was assumed to be

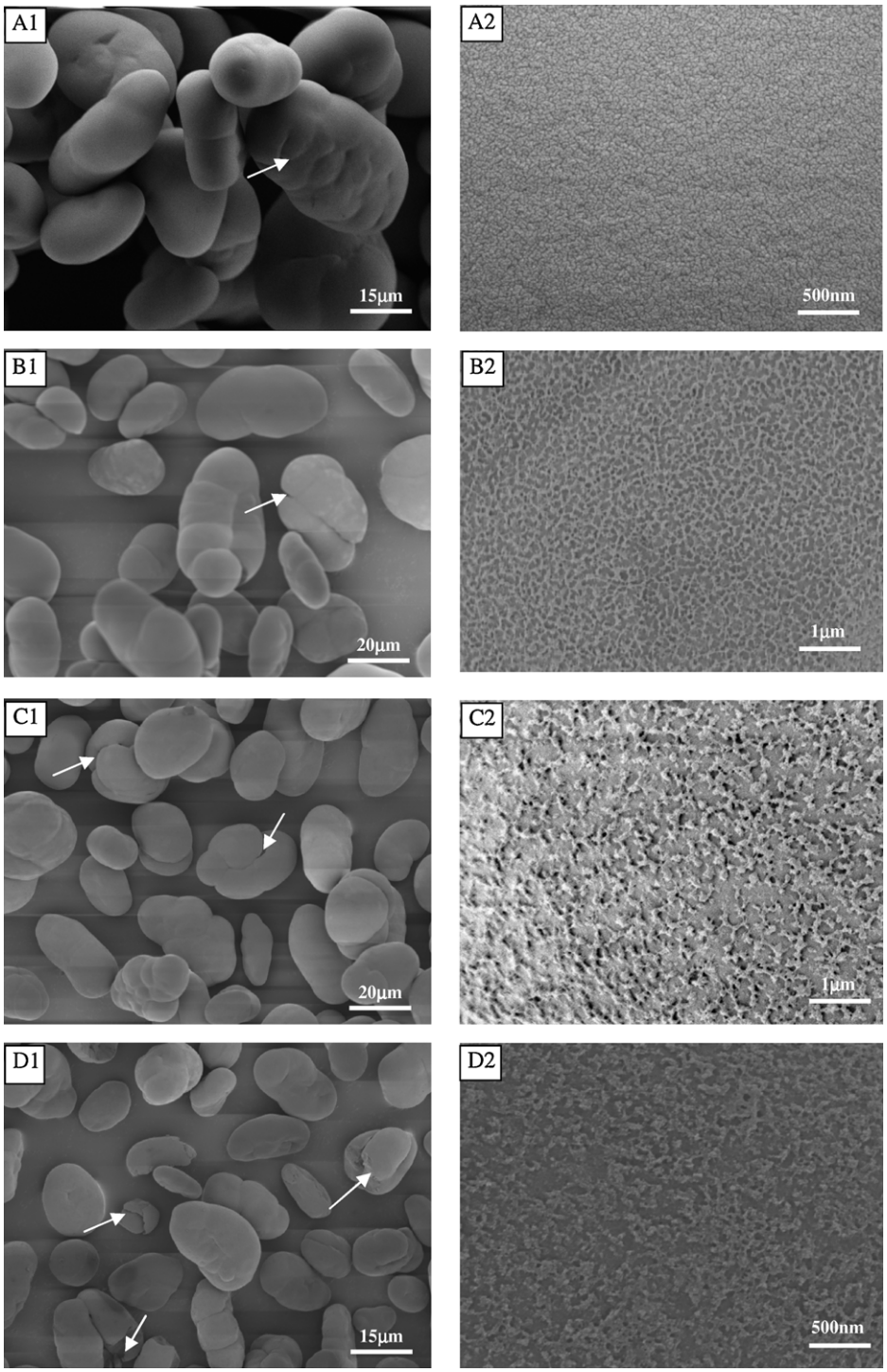

Fig. 5. Scanning electron micrographs of native starch (A1, A2), and starch residues after 1 (B1, B2), 2 (C1, C2) and 6 days (D1, D2) of hydrolysis. The arrows show grooves and indentations in the granules.

predominantly in amorphous regions. This assumption is inconsistent with the general view that amylopectin is mainly responsible for the crystallinity of native starch granules. Our observations that acid hydrolysis caused a rapid loss of both iodine and Con A binding ability of the starch provides evidence that the acid attacks amylose and amylopectin simultaneously in the initial stage of hydrolysis.

Comparison of native and partially degraded starch granules by SEM indicated that considerable damage had occurred on the granule surface after only 1 day of exposure to acid. Native granules were covered with tightly packed structures with small indentations and protrusions, which appear to correspond to the end of the amylopectin side-chain clusters grouped into nodule ('blocklet') structure (10–50 nm in diameter) as also seen by atomic force microscopy and low voltage SEM (Baldwin et al., 1997; Dang et al., 2006). These clusters were substantially eroded by acid after one day, leaving a loose, lace-like structure. The considerable damage to these structures after one day of acid hydrolysis is indicative of acid attack on amylopectin clusters in the initial stage of the hydrolysis. Such surface erosion and cracks may partly result in the increasing intensity at low q during hydrolysis. From the SEM images, together with the concomitant degradation of amylose (iodine-binding) and amylopectin (Con-A) in the initial stage of hydrolysis, we conclude

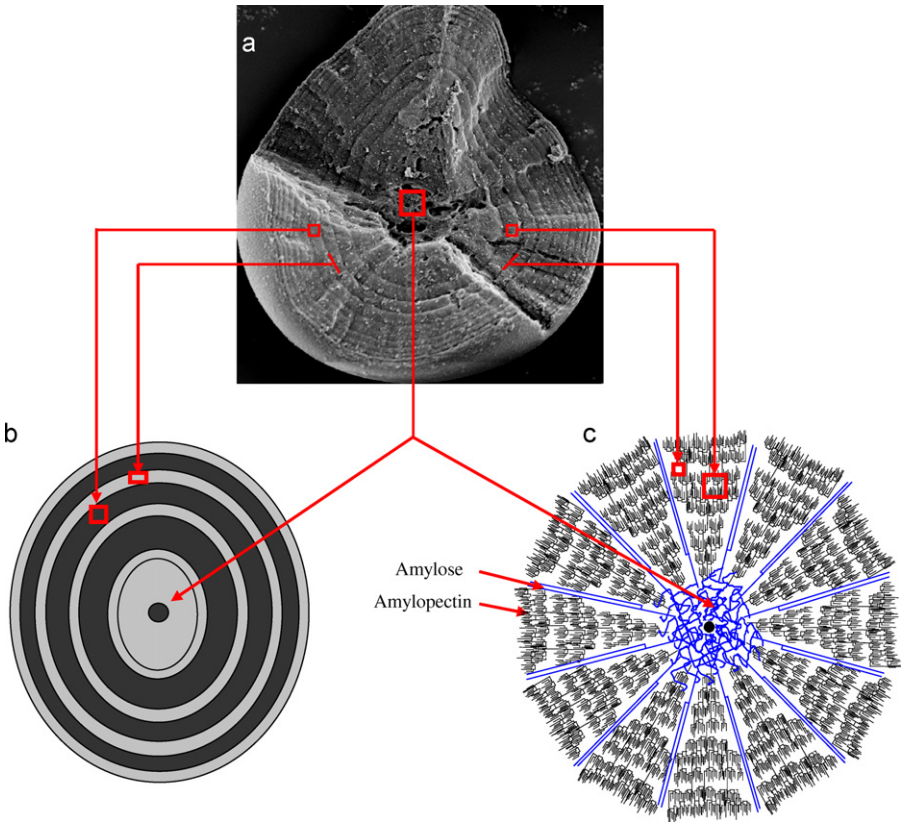

Fig. 6. Model of starch granule organization. The panels show an SEM image of a pea starch granule after 2 days of acid hydrolysis (a) and representations of a starch granule according to the growth ring model (b) and the chain distribution model (c). Panels (a) shows a split granule in cross-section; the core is seen to be extensively damaged, whereas the surrounding crystalline and amorphous rings are substantially intact. A channel from the surface to the core is clearly evident. Panels (b) and (c) depict an amorphous core surrounding the hilum composed mainly of amylose molecules and amylopectin molecules not organised into crystalline arrays. The core is surrounded by concentric semicrystalline growth rings of decreasing width towards the periphery, alternating with amorphous growth rings of more uniform thickness. The semi-crystalline growth rings are composed mainly of crystalline amylopectin interspersed with amylose molecules, whereas the amorphous growth rings are composed mainly of extended chains of amylopectin interconnecting the crystalline regions and interspersed amylose molecules. The amylose and amylopectin chains are likely to be packed more densely *in situ* than depicted.

that both types of molecules are exposed on the outer surface of granules. The major decrease in amylose content occurred between days 1 and 2, after the surface of the granules had been eroded and as a result of substantial hydrogen ions penetration into the core of the granules via channels of the type depicted in the split granule as shown in Fig. 6. This hydrolysis time also corresponds to when the maximum intensity of the B-type interhelix feature in the high q region of the SAXS is observed. The latter feature provides a signature for relative crystallinity; thus in the first 2 days, amorphous regions are hydrolyzed to an extent that the interhelix repeat is more apparent. Subsequently, double helical regions of starch are attacked also; this is presumably due to greater accessibility of the acid following initial preferential hydrolysis of the amorphous regions of the granule. This consequent extensive acid hydrolysis of amylose supports the conclusion that a substantial amount of amylose is in the core of the granules, rather than being distributed evenly throughout the granules or concentrated at the periphery, as has been suggested from some studies (Jane et al., 1992). Our conclusion is in general agreement with that of an investigation of amylose synthesis in transgenic potato starch granules, which showed that amylose is largely confined to a central region of the granule (Tatge et al., 1999).

4.2. Degradation mode of amorphous and crystalline regions

Based on a paracrystalline model for starch, Blazek and Gilbert (2010) assessed the impact of the change of a variety of model parameters on the small-angle scattering during starch digestion. They demonstrated that increases in the low q intensity can arise from digestion of the growth rings or amorphous lamellae with the latter also giving rise to corresponding increases in the lamellar peak intensity. The present study has shown that the relative crystallinity of the starch increased significantly during the first 2 days of acid hydrolysis and then increased at a slower rate between days 2 and 12. In addition, the intensity of the interhelix repeat observed in the SAXS is also at a maximum after 1 day of hydrolysis. Note that this feature is almost absent in the XRD, presumably due to the low signal-to-noise ratio. By correlating the extent of hydrolysis with the level of crystallinity at different time points used in this study, one may conclude that within the first 2 days of acid treatment predominantly amorphous material was hydrolysed. The increasing intensity of the lamellar peak near 0.6 nm^{-1} and interhelix repeat within the first 2 days indicates preferential hydrolysis of amorphous parts of the lamellae, whereas the decrease in amylose content and increasing intensity of low angle scattering are consistent with hydrolysis of other amorphous regions (amorphous growth ring and central bulk amorphous regions) although we cannot exclude the influence of supramolecular structures (blocklets, superhelices) (Blazek & Gilbert, 2010). From these data, we infer that degradation of the amorphous regions involved hydrolysis of amylose and amylopectin branch points. This deduction is consistent with the previous observations that the short, external chain fraction of amylopectin remained essentially unchanged during the initial stages of acid hydrolysis; this observation was previously interpreted as a lack of acid hydrolysis occurring initially in the crystalline lamellae (Biliaderis et al., 1981). After 2 days, hydrolysis

of both crystalline and amorphous material occurred. The disruption of crystalline lamellae at this stage is seen from the decreasing intensity of the lamellar peak, which also became broader and shifted to lower-q as interactions between amylopectin side-chains were disrupted by the acid. This is also consistent with the subsequent decrease in interhelix peak intensity. The absence of further increases in crystallinity after 12 days, and the further decrease in intensity of the lamellar peak, is consistent with hydrolysis occurring simultaneously in the crystalline and amorphous regions.

The preferential hydrolysis of amorphous lamellae was expected to result in a decrease in the lamellar d-spacing. However, it increased marginally from 10.4 to 10.8 nm within the first 2 days of hydrolysis. This small increase in d-spacing could be attributed to the reduction of constraints on semi-crystalline growth rings as a result of hydrolysis of amorphous growth rings (Waigh, Perry, Riekel, Gidley, & Donald, 1998), which could bring about a relaxation in the compact structure leading to an enlargement of the distance between crystalline and amorphous lamellae. However, extensive hydrolysis resulted in a gradual decrease of the lamellar d-spacing (from 10.8 to 9.9 nm), which is indicative of the adjacent crystalline layers coming closer together due to the hydrolysis of amorphous lamellae and partial disruption of crystalline lamellae. Thus, during the initial stage of hydrolysis, the increase in relative crystallinity is consistent with a more rapid degradation of amorphous regions, including in the core, as discussed subsequently. After the central bulk amorphous regions are substantially degraded, the relative crystallinity increased slowly and eventually leveled off, which is attributed to the hydrolysis of crystalline and amorphous regions occurring at a similar rate.

An alternative to the increasing crystallinity is that cleavage of $\alpha(1\rightarrow6)$ branch points by acid hydrolysis creates a potential for reorganisation of double helical chains. According to Waigh et al. (1998), hydrated amylopectin molecules within starch granules could behave as a liquid crystalline polymer. Decoupling of individual double helices from the amylopectin backbone could remove spatial constraints between double helices, allowing more ordered crystalline structures to form or transitions between crystal polymorphs to occur (Wang, Yu, Yu, Chen, & Pang, 2007). The dominance of the A-polymorph in acid hydrolysed starch, as shown by XRD, indicates the acid preferentially attacks the B-polymorph, resulting in its destruction, or triggering its conversion to the A-polymorph (Wang et al., 2007, 2009). Bogracheva et al. (1998) proposed on the basis of gelatinization studies that the B-polymorph is more abundant in the centre of pea starch granules, and that the A-type is more in the periphery. Our results – which show that acid hydrolysis occurs initially externally then, by penetration to the core via channels, subsequently progresses outward – provide further evidence for the proposed distribution of A- and B-polymorphs in pea starch (Bogracheva et al., 1998).

4.3. A model for the granular organization of pea starch

Our results and interpretations are consistent with a model of starch granules in which there is a central amorphous core surrounded by concentric layers of semi-crystalline growth rings and amorphous growth rings (Fig. 6). This model is based on the results from the present study and takes into account earlier models (Nikuni, 1978) as well as published electron micrographs of maize, barley, potato and pea starch granules (Li et al., 2003; Ridout et al., 2006; Wang et al., 2008a). This model proposes that the core of the granule is mainly amylose, while the outer part of the granules is predominantly composed of amylopectin interspersed with some amylose molecules (Fig. 6c). Considering the possible action of branching enzymes on these peripheral amylose chains during their biosynthesis, we suggest that these chains would have a low degree of branching. A notable feature in this model relates to the characteristics of the amorphous growth rings (Fig. 6b), which are proposed to be uniform in width according to SEM observations. The semi-crystalline growth rings, which contain organized arrays of amylopectin chains, decrease gradually in thickness towards the periphery. The distribution of amylose in this model fits well with the biosynthesis location and deposition of amylose in transgenic potato starches (Tatge et al., 1999).

5. Conclusions

The present investigation has shown that acid hydrolysis occurs within 1 day on the surface of the pea starch granules and involves both amylose and amylopectin molecules. The degradation of amylopectin occurs mainly at the α-$(1\rightarrow6)$ branch points in amorphous lamellae, as shown by the reduction in binding affinity between Con A and amylopectin. Similarly, the increased intensity of the lamellar peak is consistent with the hydrolysis of amorphous lamellae. Investigations of proton–deuteron hydroxyl groups have shown that exchange can occur rapidly within the starch granule (Ceh & Hadzi, 1958; Hennig, 1977; Khairy, Morsi, & Sterling, 1966; Taylor, Zobel, White, & Senti, 1961). Whether this is an appropriate model for the entry of hydrated protons into starch granules is not clear, but the formation of pores, cracks and fissures within 1–2 days would certainly enhance the penetration of acid into the core of the granules. This would result in promoting hydrolysis mainly in non-crystalline regions, as seen by an increase in the degree of crystallinity due to the faster degradation of amorphous regions. During this stage, the substantial reduction in amylose content and the severe damage at the core of the granules indicate that a major part of the amylose is located at the core of the granules. In the later stages of hydrolysis, the crystalline regions formed by the double helices from the short side chains of amylopectin are degraded simultaneously with the amorphous regions, as seen by only small changes in crystallinity and the decrease in lamellar peak intensity.

Summing up the known information on starch granular structure and our experimental interpretation, a new schematic model of starch granule organization is proposed in Fig. 6. Starch granules are made up of three different regions: a central amorphous region, surrounded by alternating semi-crystalline growth rings and amorphous growth rings. The semi-crystalline growth rings, which contain organized arrays of amylopectin chains, decrease gradually in thickness towards the periphery, whereas the amorphous growth rings have a similar width throughout the granule. The majority of amylose is localized at the centre of the granules, whereas the outer part of the granules is predominantly composed of amylopectin interspersed with some amylose molecules. The amorphous regions consist of bulk amylose at the centre of the granule, and amorphous growth rings that contain long linear interconnecting amylopectin chains between the crystalline amylopectin clusters, branch points of amylopectin chains organized in clusters, and interspersed amylose.

Acknowledgements

SW is the recipient of a University of Sydney Postdoctoral Research Fellowship Scheme (U2527-2009/2012). We thank technicians in the Australian Centre for Microscopy and Microanalysis for assistance with the FE-SEM and XRD, and Dr. Jinglin Yu for preparing the figures of starch granules structure using BioChemDraw software and helpful discussions.

References

Atichokudomchai, N., Varavinit, S. & Chinachoti, P. (2002). Gelatinization transition of acid-modified tapioca starches by differential scanning calorimetry (DSC). *Starch/Stärke*, *54*, 296–302.

Baldwin, P. M., Adler, J., Davies, M. C. & Melia, C. D. (1998). High resolution imaging of starch granule surfaces by atomic force microscopy. *Journal of Cereal Science*, *27*, 255–265.

Baldwin, P. M., Davies, M. C. & Melia, C. D. (1997). Starch granule surface imaging using low-voltage scanning electron microscopy and atomic force microscopy. *International Journal of Biological Macromolecules*, *21*, 103–107.

Betancur, A. D. & Chel, G. L. (1997). Acid hydrolysis and characterization of *Canavalia ensiformis* starch. *Journal of Agricultural and Food Chemistry*, *45*, 4237–4241.

Biliaderis, C. G., Grant, D. R. & Vose, J. R. (1981). Structural characterization of legume starches. II. Studies on acid-treated starches. *Cereal Chemistry*, *58*, 502–507.

Blazek, J. & Gilbert, E. P. (2010). Effect of enzymatic hydrolysis on native starch granule structure. *Biomacromolecules*, *11*, 3275–3289.

Blazek, J. & Gilbert, E. P. (2011). Application of small-angle X-ray and neutron scattering techniques to the characterization of starch structure: A review. *Carbohydrate Polymers*, *85*, 281–293.

Bogracheva, T. Y., Morris, V. J., Ring, S. G. & Hedley, C. L. (1998). The granular structure of C-type pea starch and its role in gelatinization. *Biopolymers*, *45*, 323–332.

Bogracheva, T. Y., Wang, Y. L., Wang, T. L. & Hedley, C. L. (2002). Structural studies of starches with different water contents. *Biopolymers*, *64*, 268–281.

Buléon, A., Colonna, P., Planchot, V. & Ball, S. (1998). Mini review. Starch granules: structure and biosynthesis. *International Journal of Biological Macromolecules*, *23*, 85–112.

Buléon, A., Pontoire, B., Riekel, C., Chanzy, H., Helber, W. & Vuong, R. (1997). Crystalline ultrastructure of starch granules revealed by synchrotron radiation microdiffraction mapping. *Macromolecules*, *30*, 3952–3954.

Cairns, P., Bogracheva, T. Y., Ring, S. G., Hedley, C. L. & Morris, V. J. (1997). Determination of the polymorphic composition of smooth pea starch. *Carbohydrate Polymers*, *32*, 275–282.

Ceh, M. & Hadzi, D. (1958). Die Austauschfahigkeit der Hydroxylgruppen von frischen und gealterten Amylosen bzw. Amylopektin mit schwerem Wasser. *Starch/Stärke*, *10*, 99–103.

Colonna, P., Biton, V. & Mercier, C. (1985). Interaction of concanavalin A with α-D-glucans. *Carbohydrate Research*, *137*, 151–166.

Dang, J. M. C., Braet, F. & Copeland, L. (2006). Nanostructural analysis of starch components by atomic force microscopy. *Journal of Microscopy*, *224*, 181–186.

Goldstein, I. J., Hollerman, C. E. & Merrick, J. M. (1965). Protein-carbohydrate interaction. I. The interaction of polysaccharides with Concanavalin A. *Biochimica et Biophysica Acta*, *97*, 68–76.

Hennig, H. J. (1977). Accessibilitat der Hydroxylgruppen in Starke fur Deuteriumoxid. *Starch/Stärke*, *9*, 289–328.

Hoover, R. (2000). Acid-treated starches. *Food Reviews International*, *16*, 369–392.

Jane, J. L. & Shen, J. J. (1992). Internal structure of the potato starch granule revealed by chemical gelatinization. *Carbohydrate Research*, *247*, 279–290.

Jane, J. L., Xu, A., Radosavljevic, M. & Seib, P. A. (1992). Location of amylose in normal starch granules. I. Susceptibility of amylose and amylopectin to cross-linking reagents. *Cereal Chemistry*, *69*, 405–409.

Jenkins, P. J. & Donald, A. M. (1995). The influence of amylose on starch granule structure. *International Journal of Biological Macromolecules*, *17*, 315–321.

Jenkins, P. J. & Donald, A. M. (1997). The influence of acid hydrolysis on native starch granule structure. *Starch/Stärke*, *49*, 262–267.

Khairy, M., Morsi, S. & Sterling, C. (1966). Accessibility of starch by deuteration. *Carbohydrate Research*, *3*, 97–101.

Le Corre, D., Bras, J. & Dufresne, A. (2010). Starch nanoparticles: A review. *Biomacromolecules*, *11*, 1139–1153.

Li, J. H., Vasanthan, T., Hoover, R. & Rossnagel, B. G. (2003). Starch from hull-less barley: Ultrastructure and distribution of granule-bound proteins. *Cereal Chemistry*, *80*, 524–532.

Li, W. D., Corke, H. & Beta, T. (2007). Kinetics of hydrolysis and changes in amylose content during preparation of microcrystalline starch from high-amylose maize starches. *Carbohydrate Polymers*, *69*, 398–405.

Lopez-Rubio, A., Flanagan, B. M., Gilbert, E. P. & Gidley, M. J. (2008). A novel approach for calculating starch crystallinity and its correlation with double helix content: A combined XRD and NMR study. *Biopolymers*, *89*, 761–768.

Nikuni, Z. (1978). Studies on starch granules. *Starch/Stärke*, *30*, 105–111.

Oostergetel, G. T. & van Bruggen, E. F. J. (1989). On the origin of a low angle spacing in starch. *Starch/Stärke*, *41*, 331–335.

Pérez, S. & Bertoft, E. (2010). The molecular structures of starch components and their contribution to the architecture of starch granules: A comprehensive review. *Starch/Stärke*, *62*, 389–420.

Ridout, M. J., Parker, M. L., Hedley, C. L., Bogracheva, T. Y. & Morris, V. J. (2006). Atomic force microscopy of pea starch: Granule architecture of the *rug3-a*, *rug4-b*, *rug5-a* and *lam-c* mutants. *Carbohydrate Polymers*, *65*, 64–74.

Robin, J. P., Mercier, C., Charbonniere, R. & Guilbot, A. (1974). Lintnerized starches. Gel filtration and enzymatic studies of insoluble residues from prolonged acid treatment of potato starch. *Cereal Chemistry*, *51*, 389–406.

Stevenson, D. G., Domoto, P. A. & Jane, J. L. (2006). Structures and functional properties of apple (*Malus domestica* Borkh) fruit starch. *Carbohydrate Polymers*, *63*, 432–441.

Tatge, H., Marshall, J., Martin, C., Edwards, E. A. & Smith, A. M. (1999). Evidence that amylose synthesis occurs within the matrix of the starch granules in potato tubers. *Plant, Cell and Environment*, *22*, 543–550.

Taylor, N. W., Zobel, H. F., White, M. & Senti, F. R. (1961). Deuterium exchange in starches and amylose. *Journal of Physical Chemistry*, *65*, 1816–1820.

Waigh, T. A., Hopkinson, I. & Donald, A. M. (1997). Analysis of the native structure of starch granules with X-ray microfocus diffraction. *Macromolecules*, *30*, 3813–3820.

Waigh, T. A., Perry, P., Riekel, C., Gidley, M. J. & Donald, A. M. (1998). Chiral side-chain liquid-crystalline polymeric properties of starch. *Macromolecules*, *31*, 7980–7984.

Wang, S. J. & Copeland, L. (2011). Nature of thermal transitions of native and acid-hydrolysed pea starch: Does gelatinization really happen? *Carbohydrate Polymers*, doi:10.1016/j.carbpol.2011.09.047

Wang, S. J., Sharp, P. & Copeland, L. (2011). Structural and functional properties of starches from field peas. *Food Chemistry*, *126*, 1546–1552.

Wang, S. J., Yu, J. L., Chen, W. P. & Liu, H. Y. (2008). Characterization and preliminary lipid-lowering evaluation of starch from Chinese yam. *Food Chemistry*, *108*, 176–181.

Wang, S. J., Yu, J. L. & Yu, J. G. (2008a). The semi-crystalline growth rings of C-type pea starch granule revealed by SEM and HR-TEM during acid hydrolysis. *Carbohydrate Polymers*, *74*, 731–739.

Wang, S. J., Yu, J. L. & Yu, J. G. (2008b). Conformation and location of amorphous and semi-crystalline regions in C-type starch granules revealed by SEM, NMR and XRD. *Food Chemistry*, *110*, 39–46.

Wang, S. J., Yu, J. L., Yu, J. G., Chen, H. X. & Pang, J. P. (2007). The effect of acid hydrolysis on morphological and crystalline properties of Rhizoma *Dioscorea* starch. *Food Hydrocolloids*, *21*, 1217–1222.

Wang, S. J., Yu, J. L., Yu, J. G., Chen, H. X., Pang, J. P. & Liu, H. Y. (2008). Partial characterization of starches from *Dioscorea opposita* Thunb. cultivars. *Journal of Food Engineering*, *88*, 287–293.

Wang, S. J., Yu, J. L., Zhu, Q. H., Yu, J. G. & Jin, F. M. (2009). Granular structure and allomorph position in C-type Chinese yam starch granule revealed by SEM, C-13 CP/MAS NMR and XRD. *Food Hydrocolloids*, *23*, 426–433.

Williams, P. C., Kuzina, F. D. & Hlynka, I. (1970). A rapid calorimetric procedure for estimating the amylose content of starches and flours. *Cereal Chemistry*, *47*, 411–420.

Ziegler, G. R., Creek, J. A. & Runt, J. (2005). Spherulitic crystallization in starch as a model for starch granule initiation. *Biomacromolecules*, *6*, 1547–1554.